THE JOURNAL OF PHYSICAL CHEMISTRY B LETTERS

2005, *109,* 24215−24219
Published on Web 12/01/2005

Iron Silicide Root Formation in Carbon Nanotubes Grown by Microwave PECVD

Joseph F. AuBuchon,† Chiara Daraio,† Li-Han Chen, Andrew I. Gapin, and Sungho Jin*

Materials Science and Engineering Program, Mechanical and Aerospace Engineering Department, University of California - San Diego, La Jolla, California 92093-0411

Received: October 13, 2005; In Final Form: November 15, 2005

Aligned carbon nanotubes have been grown using microwave plasma enhanced chemical vapor deposition (PECVD). The carbon nanotubes are nucleated from iron catalyst particles which, during growth, remain adherent to the silicon substrates. By analysis with high-resolution electron microscopy, we observe iron silicide roots penetrating into the silicon substrate at the interface of the catalyst particles and the substrate, thus providing strong adhesion of the carbon nanotubes onto the substrate. The iron silicide roots assist in the attachment of the catalyst particles to the substrate and play a role in the evolution of the catalyst particle morphology and resulting base growth mode. Carbon nanotubes grown by microwave PECVD could exhibit superior electrical and thermal transport properties over other PECVD processes, so an understanding of the growth mechanism is important for utilization in device applications.

I. Introduction

Carbon nanotubes (CNTs) have been widely studied for a variety of applications, mainly due to the exceptional electrical and mechanical properties that they possess.[1,2] Their use has already been demonstrated in field emission devices,[3] nanoscale electromechanical actuators,[4] field-effect transistors (FETs),[5] CNT based random access memory (RAM),[6] atomic force microscope (AFM) probes,[7] and many others.

Although much work with CNTs has been done, it is still a considerable challenge to synthesize CNTs in a desired morphology and on a large scale. Since their discovery by arc discharge over a decade ago[8] many groups have attempted to take on this challenge. The arc discharge technique was refined[9] and subsequently led to alternative processing techniques such as laser evaporation[10] and pyrolysis of hydrocarbon gases.[11] These methods had some control over the morphology of the resulting CNTs, but offered very little feasibility for large scale production with control of structure and low cost. Due to these limitations, gas-phase reactions such as chemical vapor deposition (CVD) have received the greatest attention.

Thermal CVD processes for synthesis of CNTs are relatively simple and offer reasonable uniformity, high yield, and low cost. However, the CNT alignment is generally difficult to achieve by thermal CVD (except by a crowding mechanism). Plasma enhanced chemical vapor deposition (PECVD) has constituted a large subset of the CVD processes used to grow well aligned CNTs. Several groups have demonstrated the growth of vertically aligned CNTs using direct current (dc) PECVD.[12−14] These results not only produced CNTs in reasonable amounts and with a decent uniformity, but they also had the CNTs uniformly aligned perpendicular to a substrate surface due to the applied field or electrical self-bias field created by the plasma environment. Other growth morphologies, such as bent[15] and zigzag,[16] have also been synthesized by dc PECVD. The growth of CNTs in a microwave PECVD system has been demonstrated by several groups[17−20] but is much less common than the other forms of PECVD or thermal CVD processes. While Bower et al. used a cobalt (Co) catalyst,[18] most of the published literature on CNTs grown by microwave PECVD reports the use of iron (Fe) as the growth catalyst.

While the microwave plasma enhanced CVD has been less frequently utilized for CNT growth as compared with dc PECVD or thermal CVD, presumably due to the complexity of the microwave system, the CNTs grown by microwave PECVD offer a potentially advantageous structure in terms of higher thermal and electrical conductivities for electronic applications such as vertical interconnects. Their graphene walls are more parallel to the nanotube axis as compared to the dc plasma CNTs with inclined graphene walls typical of the herringbone structure. It is therefore useful to understand the nucleation and growth of carbon nanotubes as well as their adhesion behavior in the microwave PECVD process. Understanding of the nature of CNT adhesion and the possible ways to control the adhesion are also important as the stability of attachment is also related to the stability of electrical connection and thermal conduction behavior, in addition to the mechanical stability aspect.

It is well known that there are two distinct growth modes for a CNT synthesized from catalyst particles. In the base-growth mode, the catalyst can remain on the substrate and be at the base of the growing CNT. In the tip-growth mode, the catalyst particle lifts off of the substrate and stays at the tip of the growing CNT. Some effort has been made in understanding which growth mode will occur,[21−22] but these reports are specific to adjusting certain processing conditions in a particular type of growth method and are not as applicable to other growth methods. For various applications, it is desirable to be able to control whether tip or base growth will occur. For example, if

* Corresponding author. E-mail: jin@ucsd.edu.
† These authors contributed equally.

10.1021/jp0558627 CCC: $30.25

the catalyst particle is used to guide the growth direction and create various morphologies, as in refs 15 and 16, then tip growth is desired; however, if the CNTs are being grown to serve as a thermal transfer medium (heat sink), then the strong attachment to the substrate usually associated with base growth is desired.

For the case of CNTs grown in a microwave PECVD system with Fe catalysts, both base growth[17,20] and tip growth[19] have been reported under similar growth conditions. The reports of base growth speculate that the higher deposition temperature somehow encourages anchoring of the catalyst and promotes base growth, but a further analysis of this anchoring has yet to be done. In this letter, we add to the understanding of how such catalyst anchoring can occur by reporting the base growth of aligned CNTs in a microwave PECVD system utilizing Fe as the catalyst and analyzing the formation of FeSi roots at the interface between the Fe catalyst particles and the Si substrate.

II. Experimental Section

The CNTs in this work were grown in a microwave plasma enhanced CVD system with a 2.45 GHz, 5 kW microwave power supply. Inside of a 15 cm inner diameter stainless steel cylindrical chamber, a molybdenum substrate stage was inductively heated by an internal radio frequency graphite heater underneath that provided control of the substrate temperature independent of the plasma power. Before CVD processing, a thin film of Fe (4−12 nm thickness) was deposited by electron beam evaporation onto n-type Si (100) substrates. We made no effort to remove the native oxide on the Si wafers. The samples were transferred in air to the growth chamber and heated to 800 °C in flowing hydrogen (H_2) at a pressure of 20 Torr. Upon heating, the Fe thin film breaks up and agglomerates into islands with a size distribution related to the initial thin film thickness. After heating, a 1 kW microwave plasma was formed above the sample and the atmosphere was replaced with a mixture of ammonia (NH_3) flowing at 150 cm^3/min and acetylene (C_2H_2) flowing at 50 cm^3/min with the total pressure continuing to be held at 20 Torr. The CNTs grew under these conditions until the plasma was shut off after 30 to 60 s and the samples were cooled under flowing H_2.

For microstructural analysis, scanning electron microscopy (SEM) was performed in a Philips field emission SEM. Cross sectional high-resolution transmission electron microscopy (HRTEM) was performed on a JEOL 3010 transmission electron microscope (TEM) operated at 300 kV. Nanodiffraction analysis was performed on the CNT roots in convergent beam electron diffraction (CBED) mode.

For cross sectional TEM analysis, two of the Si substrates with CNTs grown on their surfaces were sandwiched and glued on top of each other with M-bond epoxy, then sliced with a diamond saw and inserted a Teflon tube. The tube was then sliced again into thin cross-sections and the slices were grinded, polished, dimpled, and ion milled.

III. Results and Discussion

Following the CVD growth processing, the Si substrates were covered with a dark coating that was clearly visible to the eye. Under SEM analysis, a forest of aligned CNTs grown from a 4 nm thick Fe catalyst film with resulting CNT diameters of 40−50 nm and lengths of 10 μm on average was observed as shown in Figure 1A. This image was taken along a scratch line that was intentionally introduced after growth to allow us to see the bases of the CNTs. It is possible that the creation of such a scratch disrupts the alignment of the CNTs that remain attached to the substrate. The location of the catalyst particles is evident from the cross-sectional TEM images shown in Figure 1B. Here, the CNTs were grown from a 12 nm Fe catalyst film and the resulting CNTs had diameters of 100−200 nm and average lengths of 10 μm. Each CNT showed its Fe catalyst particle at its base, clearly indicating that under these conditions the CNTs grew under the base-growth mode. The inset in Figure 1B shows a lower magnification cross sectional TEM image where we can see that although the breaking up and agglomerating into particles of the initial catalyst thin film is random, there is still a relatively uniform particle size distribution and spacing. The CNTs resulting from the 12 nm Fe film have a larger average diameter than those resulting from the 4 nm Fe film, confirming the relationship between CNT diameter and catalyst particle size. The size distributions for these film thicknesses are similar to those that have been reported for different film thicknesses of Co.[18]

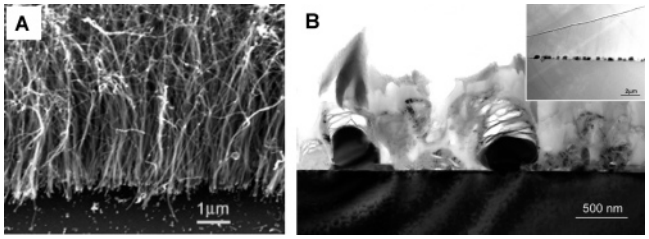

Figure 1. (A) SEM image of the as-grown CNTs. The catalyst used was a 4 nm Fe thick film deposited on Si (100). (B) Cross-sectional TEM image of CNTs grown on a 12 nm Fe catalyst film deposited on Si (100). The inset shows a low magnification overview of the interface between the Si−substrate and the catalyst particles. The catalyst particles are all located at the bases of the resulting CNTs, implicating the base-grown mode. The particle size distribution is relatively uniform and the CNT diameters appear to be larger than the one shown in (A), demonstrating the CNT's diameter-dependence on the initial film thickness.

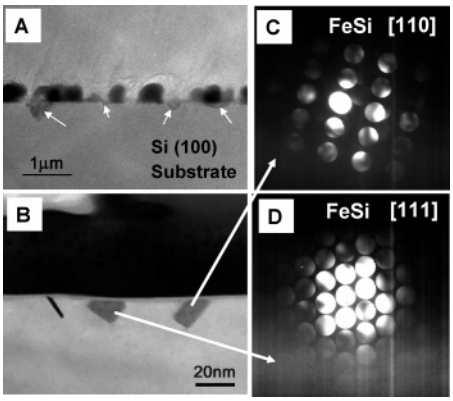

Figure 2. (A) Cross-sectional TEM image showing several catalyst particles that were formed from a 12 nm Fe film. The formation of cone and rectangular shaped structures penetrating into the Si substrate is indicated by the four small arrows. (B) High resolution TEM more clearly showing the root structures in the Si substrate. The arrows point to the zone axis nanodiffraction patterns from the corresponding particles which have been indexed and identified as FeSi shown with orientations of (C) [110] and (D) [111].

Under closer analysis of the cross sectional TEM images, we observed the formation of a new structure at the interface between the Fe catalyst particles and the Si substrate which penetrated into the Si substrate. In Figure 2A, these new structures are identified by the four small arrows. Under higher magnification, we see in Figure 2B that these new structures have a clearly different contrast and sharply defined boundaries along crystallographic planes of the single-crystal Si substrate.

The two accompanying zone axis nanodiffracion patterns in Figure 2 show that the new structures are FeSi with two different orientations of [110] and [111] for Figures 2A and 2B, respectively. Nanodiffraction is a form of convergent beam electron diffraction (CBED) that allows obtaining diffraction patterns from regions of the specimen on the order of few nanometers as opposed to conventional selected area diffraction (SAD), which is limited by a minimum area size of ~500 nm. The obtained diffraction patterns were indexed following classical electron diffraction methods.[23] The indexing was then corroborated by computer simulation, using Desktop Microscopist software.[24] FeSi was identified by choosing the best fit between the theoretically calculated *d*-spacing for different Fe_x-Si_y phases with those experimentally measured.

In a microwave PECVD system, there has already been reported evidence of the formation of a cobalt silicide ($CoSi_x$) root for base growth of CNTs.[18] In this letter, we not only report the observation of similarly shaped root structures formed in the Si substrate just below the Fe catalyst particles but we were also able to identify these structures as FeSi through their diffraction patterns. Although there has not previously been clear evidence of FeSi formation reported for microwave PECVD processes, it has been observed for the growth of CNTs in a thermal CVD process.[25−26] In these previously reported cases, however, the FeSi was primarily confined to the catalyst particles above the substrate that resulted following the break-up and agglomeration of the Fe thin film. They reported a few crater-like reaction zones in the Si substrate that were Fe rich, but for the majority of the particles, the amorphous silica layer that coats the surface of the Si substrates was not penetrated.

The growth of CNTs by a catalytic growth mechanism has been studied by many groups who usually adopt the concepts established for CVD growth of carbon fibers developed in the 1970s.[27] The believed mechanism is that CNTs grow as carbon precipitates from a supersaturated metal catalyst particle. It was also noticed early on that the activation energies for carbon filament growth from several types of metal catalysts closely resembled activation energies for carbon diffusion through the bulk of those metals.[28] This suggests that the growth rate of a CNT will be limited by the rate of carbon diffusion through its catalyst particle. The growth rate of CNTs has also been suggested to be limited by the supply of carbon from the gas phase.[29] While both of these limitations occur at the same time, depending on the situation, one of these mechanisms appears to have a more dominant effect than the other. Under thermal CVD conditions, the CNT growth rate does appear to be diffusion limited, whereas more PECVD processes appear to be gas-supply limited.

A TEM image of the base end of a CNT that has been separated from its substrate is shown in Figure 3A. The catalyst particle, which is clearly visible with its darker contrast, is cone shaped and completely encompassed by carbon. Since the CNTs are believed to precipitate from a carbon-supersaturated metal catalyst particle, we expect that this particle will actually be some Fe carbide following growth. Under CVD growth conditions, the catalyst particles are at an elevated temperature; consequently, when the catalyst particles cool off, they should precipitate carbon at their surfaces since the solubility of carbon in Fe decreases with temperature. This will reduce the amount of carbon present in the particle after growth, but not eliminate it. Another factor to consider is the incorporation of Si into the catalyst particles as was reported for thermal CVD growth.[25] The presence of Si would assist the absorption and diffusion rate of carbon as compared to pure Fe[30] and should increase

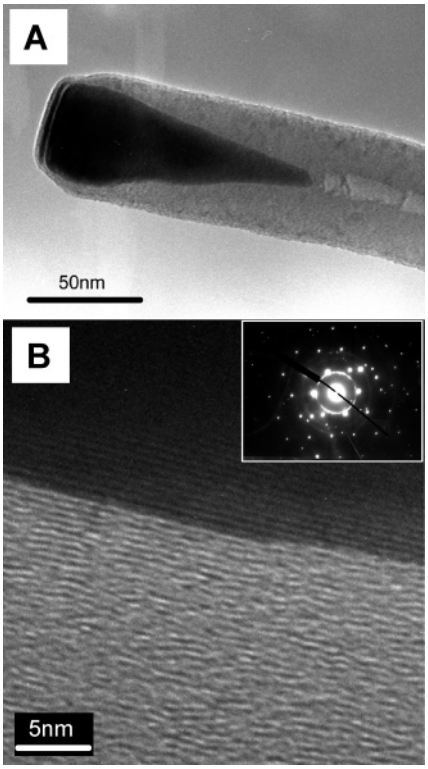

Figure 3. (A) TEM image showing the end of a CNT detached from the substrate. The catalyst particle is visible as the darker contrast, elongated, and cone-line shape inside of the CNT. It can be seen that a thin layer of carbon has completely encapsulated the catalyst particle. (B) High-resolution TEM image showing the interface between one side of a CNT and its catalyst particle. The parallel graphene planes that make up the multiwalled CNT are seen on the lower part of the image in light contrast. We can also see that the catalyst particle is crystalline in nature with atomic planes parallel to the CNT interface visible. The insert shows the diffraction pattern taken from the middle of this catalyst particle revealing that it is Fe carbide with most of it in the Fe_3C phase.

the CNT growth rate. A high resolution TEM image of the interface between one side of the CNT and the catalyst particle is shown in Figure 3B. Aligned with that interface, the parallel graphene planes which make up the multiwalled CNT can be seen. Atomic planes are also visible inside of the catalyst particle, showing a single crystal particle which is expected for a particle of such size after processing at CVD growth temperatures. The inset diffraction pattern confirms the expectations that the catalyst particle is made up Fe carbide most likely in the Fe_3C phase; however, other Fe carbide phases might exist. We did not see any evidence of Si incorporation into the catalyst particle.

The catalyst particle can have one of a number of different shapes at the end of CNT growth. The cross-sectional TEM images in Figures 4A, 4B, and 4C, shows the transition from a more equiaxially uniform catalyst particle above a flat interface with the Si substrate, to more rounded as it begins to lift its edges off from the substrate, and its eventual elongation along the CNT growth direction and total encapsulation by carbon, respectively. The catalyst particle elongation is clearly shown in Figure 3A and 4C and has been shown in all the above cited reports of CNT growth by microwave PECVD. This elongation, however, is not observed in the majority of the particles that we show in the inset of Figure 1B or in Figure 2A, both of which are cross-sectional images taken after CNT growth. It is clear that both of these competing final catalyst particle shapes are possible, but how one occurs as opposed to another is still

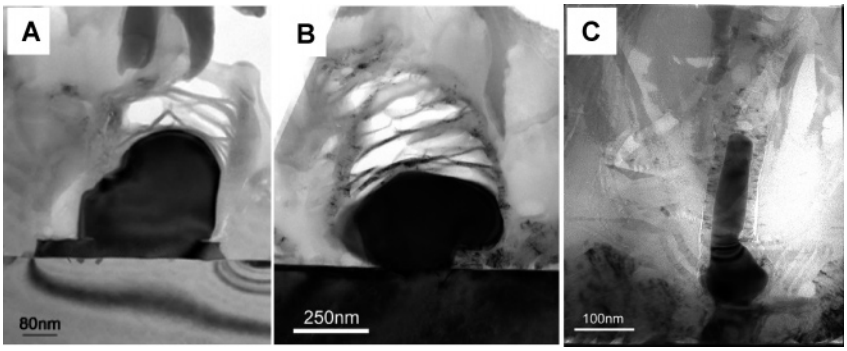

Figure 4. Series of TEM images showing various shapes that the catalyst particle can have at the end of CNT growth. Catalysts that form FeSi roots appear to be more likely to retain a large interface with the Si substrate and not allow carbon to form in that interface (A). Particles that are not as well attached to the substrate allow carbon to precipitate on their bottom surfaces and partially lift the particle off from the substrate (B) or completely encapsulate it in carbon (C). The shape of the catalyst particle can be seen elongating in the vertical direction moving from the conditions in (A) to (B) to (C). The CNTs that are normally observed in TEM that have been separated from the substrate appear most similar to (C), probably due to the ease in which these CNTs can be detached from the substrate with their catalyst particles.

not fully understood. We believe that it depends on both the initial catalyst particle size and on how strong of an attachment the initial catalyst particle made with the substrate before CNT growth began. To explain why in the literature there is a predominance of images showing elongated catalyst particles, we propose a simple explanation. Such TEM images are taken of CNTs that have been separated from their substrate and placed on another supporting grid. When removing the CNTs from their substrate, many of the catalyst particles will remain firmly attached to the substrate and have the CNT break off above them, as can be seen in the scratched area of Figure 1A. The CNTs with elongated catalyst particles, which appear to have a weaker attachment to their substrates, are able to retain their catalyst particles and these are the CNTs that we see images of. Further analysis of these pictures reveals that such images show total catalyst particle encapsulation, even across the bottom of the CNT, as shown in Figure 3A and in other sources.[18] This is an obvious indication of poor adhesion with the Si substrate and leads us to believe that there was either no formation of a root into the Si substrate or that such a root had formed but had become separated from the bulk of the catalyst particle during CNT growth.

A schematic illustration which shows the difference between the two extremes of how the final catalyst particle can be shaped is presented in Figure 5. Here the proposed sequence of events in the growth of a CNT is split into two distinct paths depending on the interaction that the catalyst particle has with the substrate. Initially a Si substrate is coated by a thin film of Fe (Figure 5A). The initial Fe catalyst thin film is heated, breaks up, and agglomerates into islands to minimize surface energies. These islands initially have a more spherical shape. Some of the islands do not interact with the substrate (Figure 5B) while some of them form FeSi roots that penetrate into the Si (Figure 5C). Once the growth stage of the CVD processing is reached (the plasma is formed over the sample and the atmosphere is changed to C_2H_2 and NH_3), the catalyst particle saturates with carbon, then precipitates carbon at its surface. Under path 1 (as labeled in Figure 5), the precipitating graphene planes form a CNT that begins to grow up from the catalyst particle, which starts to decrease its area of interface with the Si substrate as carbon is precipitated around its bottom edges (Figure 5D). Under path 2, the catalyst particle remains anchored to the substrate and carbon is unable to form beneath it (Figure 5E.) Eventually a catalyst particle in path 1 will become completely encapsulated by carbon and have an elongated shape along the CNT growth direction (Figure 5F), while the catalyst particle in path 2 retains its attachment to the Si substrate and its more equiaxed shape (Figure 5G).

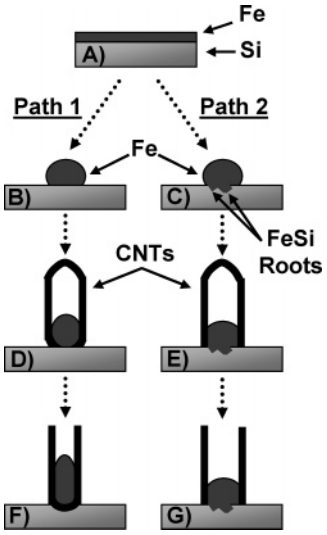

Figure 5. Schematic illustration of the proposed sequence of events in the growth of a CNT by two distinct paths. Initially a Si substrate is coated by a thin film of Fe (A). After heating, the Fe film breaks up and agglomerates into islands. Some of the islands do not interact with the substrate (B) while some of them form FeSi roots that penetrate into the Si (C). As PECVD growth processing continues, carbon precipitates at the surfaces of the catalyst particle. Under path 1, the carbon is able to begin forming under the edges of the catalyst particle and the particle decreases its area of interface with the substrate (D), while under path 2, the catalyst particle remains anchored to the substrate and carbon is unable to form beneath it (E). Eventually a catalyst particle in path 1 will become complete encapsulated in carbon and have an elongated shape along the CNT growth direction (F), while the catalyst particle in path 2 retains its attachment to the Si substrate (G).

Since we only observed the FeSi roots below particles that retained an interface with the Si substrate, we must assume that these roots assist in the attachment of the catalyst particle to the surface. This assistance appears to not only play a role in the final shape of the catalyst particle but likely contributes to the base growth mode that we observe in these CNTs. While others did report that under similar microwave PECVD growth conditions they grew CNTs with Fe catalysts in a tip growth mode,[19] two major differences were that they used a much thicker Fe catalyst film of 70 nm and added a 10 min H_2 plasma pretreatment before introducing the carbon supply gas. It could be that such a process was able to change the surface

morphology in a way that allowed particles of Fe to lift off of the surface. Even if below the Fe layer there had been formation of FeSi roots, the Fe layer would be so thick that a particle lifting off of the top surface would not be affected by such roots.

IV. Conclusion

We have analyzed the microstructure and growth mechanisms of microwave PECVD grown CNTs using Fe catalysts. The CNTs grew following a base-growth mode. At the interface between the catalyst particles and the Si substrate, we observed the formation of FeSi roots that penetrated into the Si substrate. Two possible alternative routes of catalyst−substrate interactions are proposed, which appear to play a role in the attachment of the catalyst particle to the substrate which affects the evolution of the catalyst particle shape and the occurrence of the base-growth mode. The understanding of such interactions is important for applications of CNTs grown by microwave PECVD, which can produce well aligned nanotubes, yet still exhibit less inclined graphene walls for potential advantages in terms of higher electrical and thermal conductivities as well as stronger adhesions than the more wildly investigated tip-grown and herringbone-structured CNTs made by dc PECVD.

Acknowledgment. We acknowledge support of the work by NSF NIRTs under grant numbers DMI-0210559 and DMI-0303790, and University of California Discovery Fund under Grant No. ele02-10133/Jin. We thank Dr. E. A. Stack for assistance with TEM analysis and the National Center for Electron Microscopy, Lawrence Berkeley Lab, which is supported by the U.S. Department of Energy under Contract # DE-AC02-05CH11231.

References and Notes

(1) Dresselhaus, M. S.; Dresselhaus, G.; Eklund, P. C. *Science of Fullerenes and Carbon Nanotubes*; Academic: New York, 1996.
(2) Dekker, C. *Phys. Today* **1999**, *52*, 22.
(3) Chung, D.; Park, S.; Lee, H.; Choi, J.; Cha, S.; Kim, J.; Jang, J.; Min, K.; Cho, S.; Yoon, M.; Lee, J.; Lee, C.; Yoo, J.; Kim J.; Jung, J.; Jin, Y.; Park, Y.; You, J. *Appl. Phys. Lett.* **2002**, *80*, 4045.
(4) Kim, P.; Lieber, C. M. *Science* **1999**, *286*, 2148.
(5) Tans, S.; Verschueren, A.; Dekker, C. *Nature* **1998**, *393*, 49.
(6) Rueckes, T.; Kim, K.; Joselevich, E.; Tseng, G.; Cheung, C.; Lieber, C.; *Science* **2000**, *289*, 94.
(7) Snow, E.; Campbell, P.; Novak, J. *Appl. Phys. Lett.* **2002**, *80*, 2002.
(8) Iijima, S. *Nature* **1991**, *354*, 56.
(9) Ebbesen, T. W.; Ajayan, P. M. *Nature* **1996**, *358*, 200.
(10) Qin, L. C.; Iijima, S. *Chem. Phys. Lett.* **1997**, *269*, 65.
(11) Qin, L. C. *J. Mater. Sci. Lett.* **1997**, *16* 457.
(12) Ren, Z.; Huang, Z.; Xu, J.; Wang, J.; Bush, P.; Siegal, M.; Provencio, P.; *Science* **1998**, *282*, 1105.
(13) Chen, L.-H.; AuBuchon, J. F.; Gapin, A. I.; Daraio, C.; Bandaru, P.; Jin, S.; Kim, D.-W.; Yoo, I.-K. *Appl. Phys. Lett.* **2004**, *85*, 5373.
(14) Chhowalla, M.; Teo, K.; Ducati, C.; Rupesinghe, N.; Amaratunga, G.; Ferrari, A.; Roy, D.; Robertson, J.; Milne, W. *J. Appl. Phys.* **2001**, *90*, 5308.
(15) AuBuchon, J. F.; Chen, L.-H.; Jin, S. *J. Phys. Chem. B* **2005**, *109*, 6044.
(16) AuBuchon, J. F.; Chen, L.-H.; Gapin, A. I.; Kim, D.-W.; Daraio, C.; Jin, S. *Nano Lett.* **2004**, *4*, 1781.
(17) Qin, L. C.; Zhou, D.; Krauss, A. R.; Gruen, D. M. *Appl. Phys. Lett.* **1998**, *72*, 3437.
(18) Bower, C.; Zhou, O.; Zhu, W.; Werder, J.; Jin, S. *Appl. Phys. Lett.* **2000**, *77*, 2767.
(19) Fujiwara, Y.; Takegawa, H.; Sato, H.; Maeda, K.; Saito, Y.; Kobayashi, T.; Shiomi, S. *J. Appl. Phys.* **2004**, *95*, 7118.
(20) Wang, Y. Y.; Gupta, S.; Nemanich, R. J. *Appl. Phys. Lett.* **2004**, *85*, 2601.
(21) Melechko, A. V.; Merkulov, V. I.; Lowndes, D. H.; Guillorn, M. A.; Simpson, M. L. *Chem. Phys. Lett.* **2002**, *356*, 527.
(22) Song, I. K.; Cho, Y. S.; Choi, G. S.; Park, J. B.; Kim, D. J. *Diamond Relat. Mater.* **2004**, *13*, 1210.
(23) Williams, D. B.; Carter, C. B. *Transmission Electron Microscopy* Plenum Press: New York and London, 1996; p 271.
(24) Software is available from Virtual Laboratories, Telephone 1-505-828-1640.
(25) Yao, Y.; Falk, L. K. L.; Morjan, R. E.; Nerushev, O. A.; Campbell, E. E. B. *J. Mater. Sci.: Mater. Electron.* **2004**, *15*, 533.
(26) Yao, Y.; Falk, L. K. L.; Morjan, R. E.; Nerushev, O. A.; Campbell, E. E. B. *J. Mater. Sci.: Mater. Electron.* **2004**, *15*, 583.
(27) Tibbetts, G. G. *J. Cryst. Growth* **1984**, *66*, 632.
(28) Baker, R. T. K.; Harris, P. S.; Thomas, R. B.; Waite, R. J. *J. Catal.* **1973**, *30*, 86.
(29) Merkulov, V. I.; Hensley, D. K.; Melechko, A. V.; Guillorn, M. A.; Lowndes, D. H.; Simpson, M. L. *J. Phys. Chem. B* **2002**, *106*, 10570.
(30) Baker, R. T. K.; Thomas, R. B. *J. Cryst. Growth* **1972**, *12*, 185.